Advances in Computational Hydrodynamics Applied to Wave-in-Deck Loading

***Y.L. Wu[1], G. Stewart[2], Y. Chen[1], J. Gullman-Strand[1], P. Kumar[3], X. Lv[3]**

[1]Lloyd's Register Global Technology Centre,
1 Fusionopolis Way, Connexis (North Tower) #17-14, Singapore 138632.
[2]Lloyd's Register EMEA, Aberdeen AB10 1NN, UK.
[3]Institute of High Performance Computing, Agency for Science, Technology and Research (A*STAR)
1 Fusionopolis Way, Connexis #16-16, Singapore 138632

*Corresponding author: yanling.wu@lr.org

Abstract

Owing to increases in predicted wave crest heights, platform settlement and changes to sea-water levels, wave-in-deck loading on offshore structures has increasingly become a concern to the offshore oil and gas industry. In this paper, a numerical approach for simulations of extreme ocean waves interacting with fixed offshore structures is presented in the framework of an open source library, OpenFOAM. A wave generation model based on the "NewWave" focused wave group approach (Tromans *et al*. 2001) has been developed to represent the extreme wave conditions. To validate the simulation, the results from the current approach have been compared to wave profiles obtained by Ning *et al*. (2009) and also with those of Iwanowski *et al*. (2002) for the wave-in-deck loads for a simple box representing the Ekofisk platform deck in the North Sea. The dynamic response of a typical supporting jacket structure when subjected to these loads is also assessed.

Keywords: CFD, NewWave, wave-in-deck, offshore structure, OpenFOAM

1. Introduction

Wave-in-deck loading arises when the total surface elevation exceeds the air gap for which an offshore platform has been designed. This results in very large step changes in the load on the structure and is a major concern for oil and gas operators. This situation is becoming increasingly common due to: changes in the wave crest statistical models that lead to higher crest predictions; seabed subsidence due to oil & gas extraction; and sea-level increases due to climate change.

Historically, the estimation of wave-in-deck load has mainly been conducted using semi-analytical formulations supported by laboratory experiments on scaled-down models (van de Graaf *et al*., 1995). With the advent of high powered computer clusters, numerical simulation on full size models using state-of-art CFD (Computational Fluid Dynamics) techniques now offers an alternative for determining these complicated hydrodynamics forces. The advantages of numerical simulation through CFD are: 1) full scale simulation of nonlinear phenomena; 2) potentially more accurate (and less costly) prediction compared with model testing as viscous and inertia forces are included whereas a model based on Froude scaling can only capture the inertia forces; and 3) detailed insight into the flow and resulting loads.

To evaluate wave-in-deck impact loads, an extreme wave generator needs to be employed. The extreme wave occurs as a highly transient event within a multi frequency sea state. Regular waves, such as Stokes, do not represent these extreme waves accurately and random wave generation is an extremely time consuming process, as these extreme events occur rarely in random time series. An efficient method is to use a "NewWave" focused wave group that describes the average shape of an extreme wave profile consistent with a random process and a specified energy spectrum (Tromans *et al*., 1991). NewWave theory combines random wave theory and conditional probability theory to obtain the frequency components and relative amplitudes of the wavelets of the target extreme waves. These wave components interact and constructively interfere to build up a localized extreme wave, focused at a specified position in the domain. The representation has been studied theoretically by Boccotti (1983) and Tromans *et al*. (1991) and experimentally and numerically by several investigators, such as Taylor and Haagsma (1994), Baldock *et al*. (1996) and Borthwick *et al*. (2006). In this study, we adopt the numerical setup for the generation of NewWave as published in Ning *et al*. (2009).

The NewWave model has been developed by leveraging on the open source CFD tool OpenFOAM in this study. This has an extensive range of features to solve various fluid flow problems. In the current OpenFOAM platform, the Navier-Stokes (N-S) equations are used to describe the fluid flow while the Volume of Fluid method (VOF) is used to capture movement of the water free surface.

2. Methodology and simulation

2.1 NewWave Theory

The concept of the NewWave formulation is to generate the extreme waves from a specified frequency spectrum by superimposing several relatively small waves to form one focused extreme wave at a specified location and specified time. For the linear NewWave, each wave component *i*, of frequency f_i, the amplitude a_i is defined (see for example Ning *et al*., 2009) as

$$a_i = A \frac{S(f_i)\Delta f}{\sum_i^N S(f_i)\Delta f} \tag{1}$$

where *S*(*f*) is the spectral density and Δf is the frequency step depending on the number of wave components *N* and bandwidth. *A* is the target theoretical linear wave amplitude of the focused wave. The extreme wave represented by linear NewWave theory is simply the scaled auto-correlation function corresponding to a specified spectrum.

The free surface elevation and velocity components are obtained by superposition as:

$$\begin{aligned}
\eta = \eta^{(1)} &= \sum_{i=1}^{N} a_i \cos[k_i(x-x_0) - \omega_i(t-t_0)] \\
u = u^{(1)} &= \sum_{i=1}^{N} \frac{a_i g k_i}{\omega_i} \frac{\cosh k_i(z+h)}{\cosh(k_i h)} \cos[k_i(x-x_0) - \omega_i(t-t_0)] \\
w = w^{(1)} &= \sum_{i=1}^{N} \frac{a_i g k_i}{\omega_i} \frac{\sinh k_i(z+h)}{\cosh(k_i h)} \sin[k_i(x-x_0) - \omega_i(t-t_0)]
\end{aligned} \tag{2}$$

where *z* is the vertical coordinate measured upwards from the Mean Water Level (MWL), η is the instantaneous free surface elevation, x_0, t_0 are the predefined focal location and focal time, respectively, *g* is the gravitational acceleration, *h* is the water depth, $k_i = \omega_i^2 / g \tanh(k_i h)$ is the wave number and $\omega_i = 2\pi f_i$ is the frequency. The superscript $^{(1)}$ denotes linear contributions.

For the second order NewWave [Ning *et al*. (2009), Hu *et al*. (2011) and Westphalen *et al*. (2012)], the corresponding wave elevation and velocity components *u* and *w* can be expressed as:

$$\begin{aligned} \eta &= \eta^{(1)} + \eta^{(2)} \\ u &= u^{(1)} + u^{(2)} \\ w &= w^{(1)} + w^{(2)} \end{aligned} \tag{3}$$

where $\eta^{(1)}$, $u^{(1)}$ and $w^{(1)}$ are the linear wave elevation and velocities, respectively and $\eta^{(2)}$, $u^{(2)}$ and $w^{(2)}$ correspond to the second order wave elevation and velocities, respectively. Some conflicts exist amongst different papers on 2nd order terms of Eq.(3). The details of the 2nd order terms in Eq.(3) that we derived and used in this study are given in the Appendix.

Various idealized spectra may be used to represent the sea states. The JONSWAP frequency spectrum *S*(*f*) is frequently employed (e.g. Gao *et al*. 2012) and is used herein:

$$S(f) = \beta_J H_s^2 T_p^{-4} f^{-5} \exp[-1.25(T_p f)^{-4}]\gamma_\alpha^{\exp[-(T_p f-1)^2/2\lambda^2]} \tag{4}$$

$$\beta_J \cong \frac{0.06238(1.094 - 0.01915\ln\gamma_\alpha)}{0.230 + 0.0336\gamma_\alpha - 0.185(1.9+\gamma_\alpha)^{-1}} \;;\; \lambda = \begin{cases} 0.07 & f \le f_p \\ 0.09 & f > f_p \end{cases}$$

where H_s is the significant wave height; T_p and f_p are the peak wave period and frequency respectively. The peak enhancement factor γ_α was taken as 3.3. Note that for the NewWave formulation the value of H_s is not relevant since the normalized spectrum is used (see Eq. (1)).

2.2 NewWave boundary conditions for CFD

For the boundary conditions in our CFD simulations we may use either the first order NewWave solution as given by Equation (1) or the second order NewWave solution provided by Equation (3) as the input initial conditions. In this paper, all results are generated using second order NewWave.

In general, there are two different initial conditions that can be used in the CFD simulation.

<u>Type 1 initial condition</u>: surface profile and kinematics prescribed over the entire domain
The surface profile and associate kinematics are imposed over the entire domain at t=0. At $t > 0$, the waves and kinematics are input at the boundary x = 0m.

<u>Type 2 initial condition</u>: surface profile and kinematics prescribed at inlet boundary, zero conditions over remainder of domain.
The surface profile and associate kinematics are imposed at the inlet boundary only. At t = 0, x > 0 the surface profile and kinematics are zero over the entire domain.

2.3 NewWave generation validation

The OpenFOAM solver with the NewWave generator was validated by comparison with the analytical solution and numerical results from Ning *et al*. (2009). For the numerical simulations, it was assumed that the fluid is incompressible, the surface tension on the free-surface can be ignored and the mean water depth is constant. No turbulence model was applied.

The setup was similar to the one in Ning *et al*. (2009). The computational domain was 13m long, 1m high with a water depth of 0.5m. Between x =10m and x =13m, a relaxation zone in Wave2Foam was installed to prevent reflections from the right-hand boundary. The wavemaker was located at x =0m. We note, in passing, that once the waves leave the input boundary, their propagation is controlled by fully nonlinear wave-wave interactions. We compare the CFD results with Case 2 in Ning *et al*. (2009) (as shown in Table 1) where the predefined focal point was set at $x_0 = 3m$, $t_0 = 9.2s$ and the linear input amplitude was $A = \eta_{\max}^{(1)}$ = 0.0632m. The corresponding theoretical second order amplitude at the focal point is $\eta_{\max}^{(2)}$ = 0.0677m.

Both types of initial conditions mentioned above were tested and the results were almost identical; however, Type 1 can employ a much shorter focal time because the simulation starts from an existing developed wave field and this is much more computationally efficient. Therefore, in the following, we consider only the results for initial condition Type 1.

Ning *et al*. (2009) found that due to nonlinear interaction of the NewWave components, the highest elevation (the real focus point for the wave) occurs at (x_1, t_1), where ($x_1 \geq x_0, t_1 \geq t_0$). In our study, this "focusing delay phenomenon" is investigated. Several "probe points" were set around x_0 and the position of the free surface was extracted at these positions for every time step to identify the maximum surface elevation.

Various mesh sizes were used (Table 2) to find the effect on the amplitude and real focus point location. The models were run on an HP Elitebook 8570W using 4 cores. The run times for calculation of wave propagation for 20s in time domain at coarse ($\Delta x \approx \lambda_P / 67, \Delta y \approx H/32$, $\Delta t = 0.01$), fine ($\Delta x \approx \lambda_P / 100, \Delta y \approx H/56$, $\Delta t = 0.001$), and finest mesh ($\Delta x \approx \lambda_P / 200, \Delta y \approx H/102$, $\Delta t = 0.001$) were about 2 hours, 4.5 hours and 7.5 hours, respectively. It was found that the fine mesh size ($\Delta x \approx \lambda_P / 100, \Delta y \approx H/56$, $\Delta t = 0.001$) is the optimal choice in term of accuracy and efficiency. Table 2 shows the results of the study: the real focus point occurs at (x_1, t_1) and is delayed in both time and location.

Table 1 Simulated case as per Case 2 in Ning et al., 2009

Frequency band (Hz)	Input Amplitude (m)	No. of wave components	Peak frequency (Hz)	Peak wave period T_p (s)	Characteristic wave length λ_P (m)
0.6 – 1.3	0.0632	16	0.833	1.2	2.0

Table 2 Maximum elevation and focal point comparison for different mesh size
($x_0 = 3m$, $t_0 = 9.2s$, $\eta_{\max}^{(1)} = A$ =0.0632m, $\eta_{\max}^{(2)}$ =0.0677m)

Case	Maximum elevation $\eta_{\max}$ (m)	Location of x_1(m)	Time of occurrence t_1(s)	Max crest/ linear crest, $\eta_{\max} / \eta_{\max}^{(1)}$	Max crest/ 2nd order crest, $\eta_{\max} / \eta_{\max}^{(2)}$
Coarse mesh	0.0691	4.0	9.68	1.093	1.021
Fine mesh	0.0750	3.5	9.57	1.187	1.108
Finest mesh	0.0771	3.4	9.37	1.220	1.139
Ning et al. (2009)	0.0704	3.4	9.64	1.114	1.040

Figure 1 shows the time history of surface elevation at the actual focal point obtained by the NewWave CFD simulation based on the fine mesh model (blue dashed line). The second order NewWave analytical solution is also shown for comparison (red line) and the black line is Ning *et al*.'s (2009) results. Ning *et al*. used a Higher-Order Boundary Element Method (HOBEM) with mesh size is $\Delta x \approx \lambda_P / 30$ and time step $\Delta t = T_P / 50 = 0.024$. It is clear that the surface elevations at the real focal point from both OpenFOAM and the HOBEM solver used by Ning *et al*. are higher than the analytical solution. This is because the effect of nonlinear wave-wave interactions beyond second order is not included in the analytical solution. Overall the comparison is good although the surface elevation from the N-S solver (OpenFOAM) is 6% higher than the potential flow solver used by Ning *et al*. This may be due to the different mesh size and time step, or due to the difference between N-S solver and HOBEM solver.

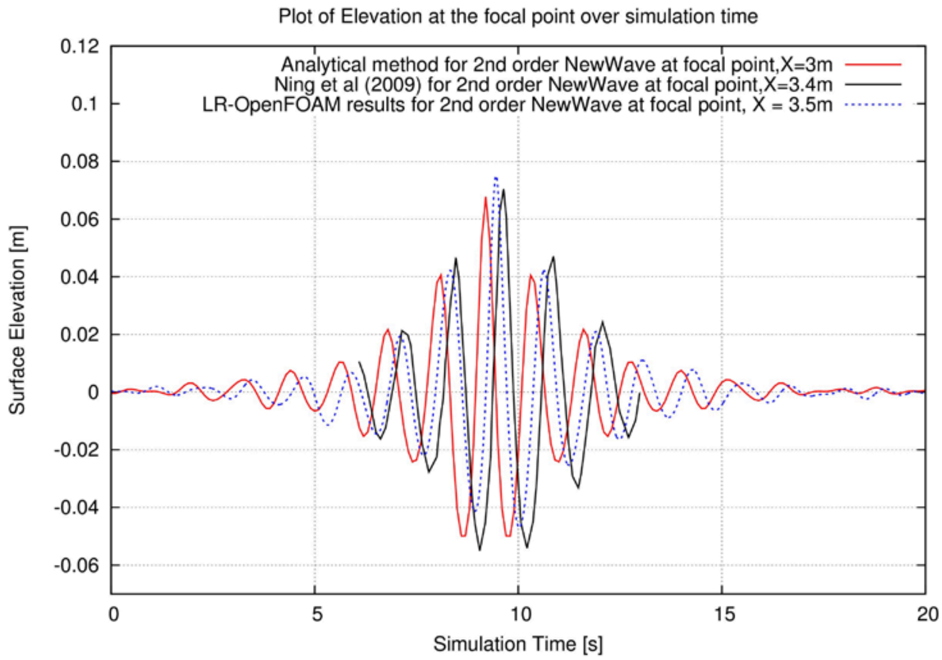

Figure 1 Comparison of wave elevations at focal points

2.4 Numerical results for Wave-in-deck simulations

Iwanowski *et al*. (2002) calculated 100 year wave-in-deck loads for a model representing the Ekofisk platform deck in the North Sea. They presented and compared load time histories calculated by several different approaches, including analytical formulations and CFD simulations. In their work, the incident wave was a regular Stokes 5th order defined by the parameters *H* (wave height), *T* (wave period), and water depth *d*. We compare their results with our NewWave CFD model - the parameters for the target focused wave are summarized in Table 3. A comparison of our CFD results with Iwanowski *et al*.'s for wave-in-deck loads for Stokes 5th order waves (Chen *et al*. 2014) is also presented. The deck was modelled as a simple box being 50m long and 10m high with wave inundation at 4m. Because this study is based on 2D simulation, the actual width of the deck being 30m (normal to the wave propagation direction) is only used in post-processing to calculate the force for comparison with Iwanowski *et al*.

For the NewWave simulation, a conversion factor of 1/0.93 was used to obtain Tp from the Stokes wave period (T). We then matched the amplitude[1] of the Stokes 5th and the simulation based on NewWave. For a Stokes 5th wave of height 24.3m the corresponding wave amplitude is 14.263m. For the Newwave CFD, the input amplitude A was adjusted to 11.91m through trial and error to get the required wave elevation 14.263m. To achieve the required wave impact height $h_{imp} = 4$ the structural model was placed 10.263m above the water free surface.

In the following simulations, the mesh size around the free surface and around the deck is $\Delta x \approx \lambda_P / 150$, $\Delta y \approx H / 50$. Type 1 initial condition was used with second order NewWave.

Table 3 Parameters of waves for the model of Iwanowski et al. (2002)

Parameter	**Stokes 5th wave**	**NewWave**
Water depth d (m)	80	80
Wave elevation E (m)	14.263	14.263 (A = 11.91)
Wave Height H (m)	24.3	22.13 for the focus wave (calculated from the numerical results)
Wave period T (sec)	14.5	T_p =(T/0.93) =15.59
Peak frequency (Hz)	-	0.06414
Frequency band in JONSWAP spectrum (Hz)	-	0.0237-0.1924 (40 components)
Wave length λ (m)	320	λ_P =320
Impact Height (h_{imp}) (m)	4	4
Predefined focal time t_0 for NewWave (s)	-	t_0 = 1.5T_p = 23.34
Predefined focal position x_0 for NewWave (m)	-	$x_0 = 1.5\lambda_P = 480$

Figures 2 and 3 show the time force curves for the horizontal force Fx and vertical force Fz for OpenFOAM NewWave 2D simulation along with the 2D results based on Stokes 5th waves. The Stokes 5th wave 2D results from Iwanowski *et al*. (2002) by FLOW3D are also compared in the figures.

1 In practice the crest height would be obtained using Forristall crest statistics (Forristall, 2000) and then NewWave and Stokes 5th waves would be selected to match that crest height.

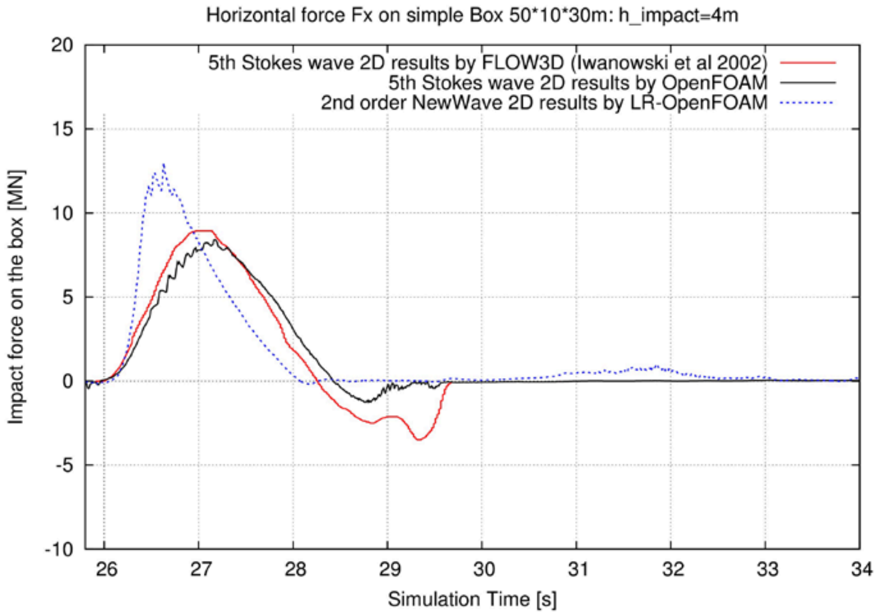

Figure 2 Comparison of horizontal force

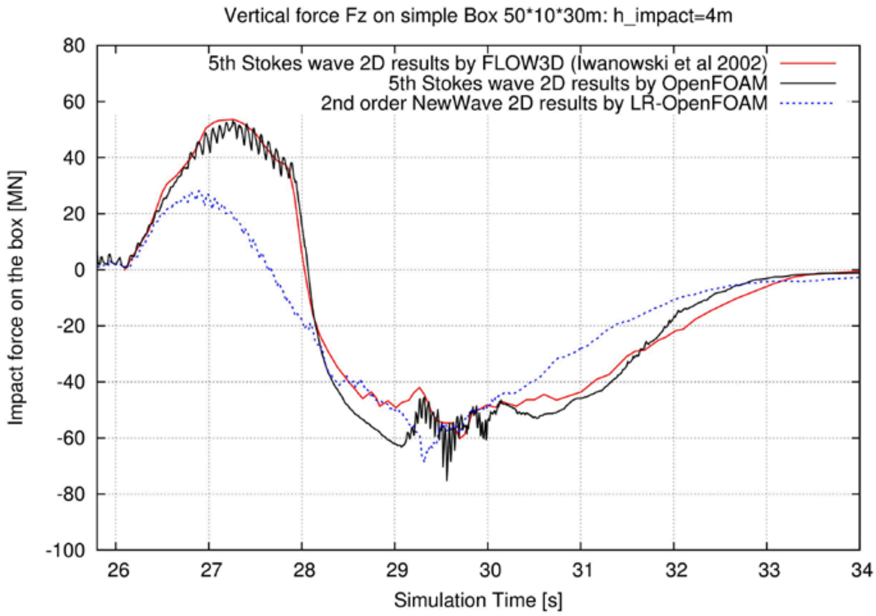

Figure 3 Comparison of vertical force

It is clear that there is good agreement between Stokes 5th wave 2D results for our OpenFOAM simulation and FLOW3D. This demonstrates that the present computational simulation is comparable with other available CFD results in the literature.

For the NewWave simulation with the same elevation as the Stokes 5th wave, it was found that the peak of horizontal force acting on the simple box for NewWave is higher than that of the Stokes 5th wave and its duration is less; however the area under the curve of the NewWave simulation (the impulse) is essentially the same as that for the Stokes 5th wave (NewWave impulse = 11.0 MNs; Stokes impulse = 10.9 MNs). In practice, one would derive the crest elevation based on Forristall crest statistics (Forristall, 2000). This study indicates that if a Stokes wave is matched to the crest amplitude, the corresponding force may be significantly underestimated compared with a NewWave with the same crest amplitude. It is therefore recommended that focused waves based on NewWave are employed in CFD simulations.

The forces obtained from our simulations are the forces on the deck without consideration of structural dynamic response. The effective force applied to the supporting jacket structure depends on the peak force, the duration of the force and the natural period of the jacket. To determine the effect of dynamics of the structure, the static force-time histories shown in Figure 2 were applied to a single degree of freedom mass-spring-damper system that represents the supporting jacket structure with a natural frequency of 2.5 secs and 3% critical damping. The input force (f_deck) and response curves (force in the jacket) are shown in Figure 4. In this case, although the overall impulse is the same, the resulting force in the jacket is greater for NewWave compared with Stokes 5^{th}. It is this dynamically enhanced force that is used for the assessment of structural integrity of the jacket structure.

From the above we note that the static wave-in-deck force is amplified by the dynamic behavior of the jacket structure resulting in higher loads being transmitted to the jacket. The NewWave *dynamic amplification factor* (DAF) is 1.39 while the Stokes 5^{th} DAF is 1.64. These are fairly typical values for a fixed jacket structure with wave-in-deck loading – the particular value depends on the applied wave-in-deck force-time history and jacket natural frequency as mentioned above.

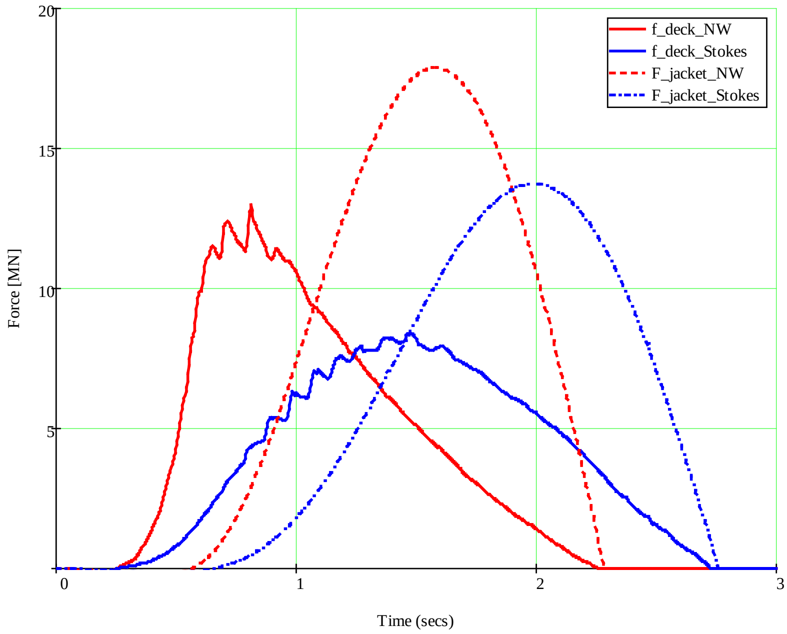

Figure 4 Lateral dynamic response of jacket structure to wave-in-deck loading
(Natural period = 2.5 secs; 3% critical damping)

For the vertical force comparison in Figure 3, there are significant differences between the NewWave and Stokes 5^{th} wave solutions. The upward vertical force Fz for NewWave is about 1/2 that of the Stokes 5^{th} wave. This is most likely due to the different wave shape and crest velocity of the different wave theories.

3. Conclusions

NewWave theory provides an efficient description of the average profile of an extreme event in a random sea. The advantage of NewWave is that the extreme wave can be generated at a predefined location and time without extensive random time domain simulations. When implemented as an initial condition into a CFD package that solves the Navier-Stokes equations, cost effective wave-in-deck loading simulations can be undertaken that include the full non-linearity of the waves.

This paper describes the development of an extreme wave generator based on second order NewWave theory that was implemented into the OpenFOAM CFD software. A comparison between NewWave and a Stokes 5th wave has been made by calculating the wave-in-deck loading on a simple box and the corresponding response of a supporting jacket structure. This study indicated that if a Stokes 5th wave is matched to the crest amplitude of NewWave, the applied horizontal deck force and the jacket response may be significantly underestimated compared to NewWave. The upward vertical forces from NewWave are substantially lower than the Stokes 5th wave. It is therefore recommended that focused waves based on NewWave are employed in CFD simulations.

Acknowledgments

Financial support provided by Lloyds Register for this work is gratefully acknowledged. And thanks Mr. Anand Bahuguni for providing the analytical solution in Figure 1 for comparison.

Disclaimer

The views expressed in this paper are those of the authors and do not necessarily reflect those of their affiliated companies.

References

Baldock T.E., Swan C., Taylor P.H. (1996): A laboratory study of nonlinear surface waves on water, Philosophical Transactions of the Royal Society of London 354A : 649-676.

Boccotti P., (1983): Some New results on Statistical properties of Wind Waves, Applied Ocean Research, Vol. 5, No. 3.

Borthwick A.G.L., Hunt A.C., Feng T., Taylor P.H., Stansby P.K. (2006): Flow kinematics of focused wave groups on a plane beach in the UK coastal research facility, Coastal Engineering 53 (12): 1033-1044.

Chen Y., Wu Y.L., Stewart G., Gullman-Strand J., and Lu X. (2014): Numerical simulation of wave in deck loading on offshore structures, OMAE2014-23847, Proceedings of the ASME 33rd International Conference on Ocean, Offshore and Arctic Engineering, June 8-13, 2014, San Francisco, California, USA.

Dalzell J.F.(1999): A note on finite depth second-order wave-wave interactions, Applied Ocean Research 21:105-111.

Forristall, G.Z. (2000): Wave crest distributions – Observations and second order theory, J. Phys Oceanog. Vol 30, No. 8: 1931-1943.

Gao F., Mingham C., and Causon D.: Simulation of extreme wave interaction with Monopile mounts for offshore wind turbines, Coastal Engineering 2012.

Hu Z.Z., Causon D.M., Mingham C.G., and Qian L.(2011): Numerical simulation of floating bodies in extreme free surface waves, Nat.Hazards Earth Syst. Sci.,11,519-527,2011

ISO 19902+A1, Petroleum and Natural Gas Industries-Fixed Steel Offshore Structures (October 2013)

Iwanowski, B., Grigorian, H., & Scherf, I. (2002). Subsidence of the Ekofisk Platforms: Wave in Deck Impact Study—Various Wave Models and Computational Methods. OMAE2002-28063, Proceedings of OMAE'02, 21st International Conference on Offshore Mechanics and Artic Engineering, June 23-28, 2002, Oslo, Norway.

Jacobsen, N. G., Fuhrman, D. R., & Fredsøe, J. (2012). A wave generation toolbox for the open source CFD library: OpenFoam®. International Journal for Numerical Methods in Fluids, 70(9), 1073-1088.

Ning D.Z., Zang J., Liu S.X., Eatock Taylor R., Teng B., Taylor P.H.(2009): Free surface evolution and wave kinematics for nonlinear uni-directional focusd wave groups, Ocean Engineering, 36:1226-1243.

Taylor P.H., Haagsma I.J.(1994): Focusing of steep wave groups on deep water, Proceedings of the International Symposium: Waves-Physical and Numerical Modelling, Vancouver, Canada, 862-870

Tromans P.S., Anaturk A.R., Hagemeijer A., (1991): A new model for the kinematics of large ocean waves-Application as a design wave, Proceeding of 1st International Offshore and Polar Engineering Conference, vol 3, Edinburgh, UK, 64-71

Van de Graaf, J.W., Tromans, P.S., Vanderschuren, L. (1995): Wave Loads on Decks. Shell Offshore Structures Engineering Newsletter, No. 10. Feb.

Westphalen J, Greaves D.M., Williams C.J.K., Hunt-Raby A.C., and Zang J. (2012): Focused waves and wave-structure interaction in a numerical wave tank, Ocean Engineering 45 9-12, 2012.

Appendix: Second order NewWave theory

For 2nd order NewWave theory (Eq (3)), the underlying equations for 2nd order terms can be derived according to second order Stokes theory (Ning *et al*. 2009), which can be written as

$$\eta^{(2)}=\sum_{i=1}^{N}\sum_{j=i+1}^{N}\{a_i a_j B^+\cos[(k_i+k_j)(x-x_0)-(\omega_i+\omega_j)(t-t_0)]+$$

$$a_i a_j B^-\cos[(k_i-k_j)(x-x_0)-(\omega_i-\omega_j)(t-t_0)]\}+ \tag{i}$$

$$\sum_{i=1}^{N}\{\frac{a_i^2 k_i}{4\tanh(k_i h)}(2+\frac{3}{\sinh^2(k_i h)})\cos[2(k_i(x-x_0)-\omega_i(t-t_0))]-\frac{a_i^2 k_i}{2\sinh(2k_i h)}\}$$

$$u^{(2)}=\sum_{i=1}^{N}\sum_{j=i+1}^{N}\{a_i a_j A^+(k_i+k_j)\frac{\cosh[(k_i+k_j)(z+h)]}{\cosh[(k_i+k_j)h]}\cos[(k_i+k_j)(x-x_0)-(\omega_i+\omega_j)(t-t_0)]+$$

$$a_i a_j A^-(k_i-k_j)\frac{\cosh(k_i-k_j)(z+h)}{\cosh(k_i-k_j)h}\cos[(k_i-k_j)(x-x_0)-(\omega_i-\omega_j)(t-t_0)]\}+ \tag{ii}$$

$$\sum_{i=1}^{N}\frac{3a_i^2 k_i\omega_i}{4}\frac{\cosh(2k_i(z+h))}{\sinh^4(k_i h)}\cos[2(k_i(x-x_0)-\omega_i(t-t_0))]$$

$$w^{(2)}=\sum_{i=1}^{N}\sum_{j>i}^{N}\{a_i a_j A^+(k_i+k_j)\frac{\sinh[(k_i+k_j)(z+h)]}{\cosh[(k_i+k_j)h]}\sin[(k_i+k_j)(x-x_0)-(\omega_i+\omega_j)(t-t_0)]+$$

$$a_i a_j A^-(k_i-k_j)\frac{\sinh[(k_i-k_j)(z+h)]}{\cosh[(k_i-k_j)h]}\sin[(k_i-k_j)(x-x_0)-(\omega_i-\omega_j)(t-t_0)]\}+ \tag{iii}$$

$$\sum_{i=1}^{N}\frac{3a_i^2 k_i\omega_i}{4}\frac{\sinh[(2k_i(z+h)]}{\sinh^4(k_i h)}\sin[2(k_i(x-x_0)-\omega_i(t-t_0))]$$

$$D^{\pm}=(\omega_i\pm\omega_j)^2-g(k_i\pm k_j)\tanh[(k_i\pm k_j)h] \tag{iv}$$

$$A^+=-\frac{\omega_i\omega_j(\omega_i+\omega_j)}{D^+}\left[1-\frac{1}{\tanh(k_i h)\tanh(k_j h)}\right]+\frac{1}{2D^+}\left[\frac{\omega_i^3}{\sinh(k_i h)^2}+\frac{\omega_j^3}{\sinh(k_j h)^2}\right] \tag{v}$$

$$A^-=\frac{\omega_i\omega_j(\omega_i-\omega_j)}{D^-}\left[1+\frac{1}{\tanh(k_i h)\tanh(k_j h)}\right]+\frac{1}{2D^-}\left[\frac{\omega_i^3}{\sinh(k_i h)^2}-\frac{\omega_j^3}{\sinh(k_j h)^2}\right] \tag{vi}$$

$$B^+=\frac{(\omega_i{}^2+\omega_j{}^2)}{2g}-\frac{\omega_i\omega_j}{2g}\left[1-\frac{1}{\tanh(k_i h)\tanh(k_j h)}\right]\cdot\left[\frac{(\omega_i+\omega_j)^2+g(k_i+k_j)\tanh((k_i+k_j)h)}{D^+}\right]$$
$$+\frac{(\omega_i+\omega_j)}{2gD^+}\left[\frac{\omega_i^3}{\sinh(k_i h)^2}+\frac{\omega_j^3}{\sinh(k_j h)^2}\right] \tag{vii}$$

$$B^-=\frac{(\omega_i{}^2+\omega_j{}^2)}{2g}+\frac{\omega_i\omega_j}{2g}\left[1+\frac{1}{\tanh(k_i h)\tanh(k_j h)}\right]\cdot\left[\frac{(\omega_i-\omega_j)^2+g(k_i-k_j)\tanh((k_i-k_j)h)}{D^-}\right]$$
$$+\frac{(\omega_i-\omega_j)}{2gD^-}\left[\frac{\omega_i^3}{\sinh(k_i h)^2}-\frac{\omega_j^3}{\sinh(k_j h)^2}\right] \tag{viii}$$